The variation of the particle number size distribution during the rainfall: wet scavenging and air masses changing

Guangdong Niu[1], Ximeng Qi[1,2], Liangduo Chen[1], Lian Xue[1,2], Shiyi Lai[1], Xin Huang[1,2], Jiaping Wang[1,2], Xuguang Chi[1,2], Wei Nie[1,2], Veli-Matti Kerminen[3], Tuukka Petäjä[3], Markku Kulmala[3] and Aijun Ding[1,2]

[1]Joint International Research Laboratory of Atmospheric and Earth System Sciences, School of Atmospheric Sciences, Nanjing University, Nanjing, China.

[2]Jiangsu Provincial Collaborative Innovation Center for Climate Change, Nanjing University, Nanjing, China.

[3]Institute for Atmospheric and Earth Systems Research/Physics, Faculty of Science, University of Helsinki, Helsinki, Finland.

Correspondence to: Ximeng Qi (qiximeng@nju.edu.cn)

Abstract. Below-cloud wet scavenging is an important pathway to remove atmospheric aerosols. The below-cloud wet scavenging coefficient (BWSC) is the value to describe the ability of rainfall to remove aerosols. The reported BWSCs obtained from the field measurements are much higher than the theory, but the reason for this remains unclear. Based on the long-term field measurements in the Yangtze River Delta of eastern China, we find that 28% of the rainfall events are high BWSC events. The high BWSC events show the sudden decrease of particle number concentration in all size bins near the end of rainfall. By investigating the simultaneously observed changes in carbon monoxide and aerosol chemical compositions during rainfall events, the circulation patterns and backward trajectories, we find the cause of the high BWSC events is the air masses changing but not the wet scavenging. The change of air masses is always followed by the rainfall processes and cannot be screened out by the traditional meteorological criteria, which would cause the overestimation of BWSC. After excluding the high BWSC events, the observed BWSC is close to the theory and is correlated with the rainfall intensity and particle number concentrations prior to rainfall. This study highlights that the discrepancy between the observed BWSC and the theoretical value may not be as large as it is currently believed. To obtain reasonable BWSCs and parameterization from field measurements, the effect of air masses changing during rainfall needs to be carefully considered.

1 Introduction

Atmospheric aerosols significantly impact human life by affecting air quality and climate change (Atkinson et al., 2014;Heal et al., 2012;IPCC, 2021;Rosenfeld et al., 2019). The particle number concentration, as well as their size distribution (i.e. particle number size distribution), are the main physical properties that determine the environmental and climate effects of aerosol particles (Asmi et al., 2011;Chen et al., 2021;Qi et al., 2015;Xausa et al., 2018). The epidemiological studies show that particle number concentration is highly related to human health effects (Chen et al., 2016;Downward et al., 2018;Knibbs et al., 2011). Additionally, only the particles with a size larger than the critical diameter (~50–100 nm) can act as the cloud condensation nuclei, which further alter the cloud properties and thereby the Earth's radiative balance (Kerminen et al., 2012;Schmale et al., 2018;Shen et al., 2019;Twomey, 1991).

The competition between sources and sinks of particles determines the aerosol number concentration, which can be reflected in the variation of particle number size distribution. Many studies focus on the sources of particles, while the studies on the sinks of particles are limited (Calvo et al., 2013;Daellenbach et al., 2020;Li et al., 2016;Zhang et al., 2018). Wet deposition is one of the most important sinks for particles (Hou et al., 2018;Textor et al., 2006;Wang et al., 2021), which can be separated into two types, i.e. below-cloud wet scavenging and in-cloud wet scavenging (Tinsley et al., 2000;Zhao et al., 2015). Earlier studies concluded that below-cloud wet scavenging was negligible compared to in-cloud wet scavenging and, thus, was not considered in many global models (Stier et al., 2005;Textor et al., 2006). However, for the polluted region, the below-cloud wet scavenging can be the main sink of particles within the planetary boundary layer and should not be ignored (Ge et al., 2021;Xu et al., 2017). The below-cloud wet scavenging is that raindrops capture particles through Brownian diffusion, inertial impaction, interception, thermophoresis and electrical charge effects (Seinfeld and Pandis, 2016). Those below-cloud wet scavenging mechanisms are size-dependent: Brownian diffusion and electrical charge effects are efficient for the particles with size below ~200 nm, while for coarse mode aerosols, inertial impaction and interception are the main removal mechanism (Chate and Pranesha, 2004;Greenfield, 1957;Seinfeld and Pandis, 2016). The size-dependent scavenging mechanisms lead to weak below-cloud wet scavenging in the 200-2000 nm size range, which is the so-called "Greenfield gap" (Greenfield, 1957). This Greenfield gap is related to the rainfall type, rainfall intensity, and aerosol properties (Chate, 2005).

The below-cloud wet scavenging coefficient (BWSC) is the parameter that describes the ability of rainfall to remove particles. Studies on BWSCs based on field observations in different environments are limited (Blanco-Alegre et al., 2018;Chate and Pranesha, 2004;Cugerone et al., 2018;Laakso et al., 2003;Maria and Russell, 2005;Wang et al., 2014;Xu et al., 2019;Zhao et al., 2015;Zikova and Zdimal, 2016). Xu et al. (2019) conducted field measurements in Beijing of China, and found that the BWSCs calculated by multiple methods are consistent. Zhao et al. (2015) compared the removal effects of thunderstorm rain with those of non-thunderstorm rain and found that non-thunderstorm rain was more effective in removing particles below 500 nm, while thunderstorm rain had more effective removal of particles between 500-1000 nm. However, most of the studies have limited datasets with only few rainfall events so that the role of meteorological condition change and instantaneous emission change cannot be ruled out. Some studies collected long-term field measurement datasets to calculate the scavenging coefficient by using various

selection criteria to screen the effects of other factors (Laakso et al., 2003;Roy et al., 2019;Zikova and Zdimal, 2016). Roy et al. (2019) used a long-term field observation dataset to investigate the below-cloud wet scavenging in the eastern Himalaya and found threshold values for the removal effect in terms of rain rate and duration. Laakso et al. (2003) calculated the below-cloud wet scavenging coefficient based on long-term observations of particle number size distribution (PNSD) in boreal forest of Finland and analyzed the dependence of BWSC on rainfall intensity. All those studies found that the BWSCs calculated from the field measurements were much higher than those from the theoretical estimations and model simulations in the "Greenfield gap" range. Bae et al. (2010) added electric charging and phoretic effects in the model but still cannot simulate the observed high BWSCs. Until now, the reasons for the large discrepancy between the BWSCs derived from field measurements and theory remain unclear, which limits the simulations of aerosol budget.

Yangtze River Delta (YRD) of eastern China is one of the largest city clusters in the world (Kulmala et al., 2021). Because of rapid urbanization and industrialization, the YRD area has been suffering from severe air pollution (Ding et al., 2013;Ming et al., 2017;Xie et al., 2015). Meanwhile, located in regions strongly affected by the East Asian monsoon, rainfall events of various intensities are frequent. Long-term field measurements in the YRD area would provide an ideal opportunity to explore how rainfall removes atmospheric aerosols in polluted environments. In this study, based on the seven-year measurements at the SORPES station in YRD of eastern China, we investigated variations of PNSD during rainfall processes. The aims of this study are: 1) to understand the characteristics of BWSC in polluted environments, 2) to explain the large discrepancy between observed and theoretical BWSC, and 3) to analyze the key factors affecting BWSC in ambient environments.

2 Methods

2.1 Measurement site and data

The long-term field measurements were conducted at the SORPES station (118°57′10′′E, 32°07′14′′N). The SORPES station is located about 20 km northeast of downtown Nanjing which can be considered a suburban station, and is regarded as a regional background station in the YRD region of eastern China (Ding et al., 2013). YRD region is located in the lower reaches of the Yangtze River and has abundant rainfall, especially during the "plum rain season" (June–July). Seasonal variations of monthly accumulated precipitation and rainfall frequency (ratio of the number of monthly rainfall events to the total number of rainfall events) at SORPES from 2012–2018 are shown in Fig. 1a. It could be seen that the accumulated precipitation and rainfall frequency are high in the YRD region, with June-August being particularly prominent. Certain number of rainfall events provide sufficient episodes to investigate the below-cloud wet scavenging. In addition, the SORPES station is heavily equipped with the instruments for measuring the meteorology and atmospheric components, including aerosols, trace gases and relevant meteorological parameters. More details about the SORPES station can be found in Ding et al. (2016).

The PNSDs from 6 nm to 800 nm were observed by the Differential mobility particle sizer (DMPS) (Qi et al., 2015). The time resolution of PNSD data was 10 minutes, and the data from 2012 to 2018 were used. The PNSDs data were

subjected to data quality control, and the available data number used in this study was 1793 days. The shaded area in Fig. 1b shows the median PNSD at the SORPES station from 2012 to 2018, demonstrating a multimodal distribution caused by the various sources of particles (Chen et al., 2021;Qi et al., 2015). About 382 rainfall events were recorded when the PNSD data was available. The red and green lines in Fig. 1b are the median PNSD one hour before and after the rainfall events. The PNSD before rainfall events is similar to the total median PNSD, while the number concentration in each size bin shows various degrees of decrease after the rainfall. The decrease in the particle number concentration after rainfall implies that notable variation of PNSD during the rainfall events and the below-cloud wet scavenging could be a vital sink of aerosols in the YRD region.

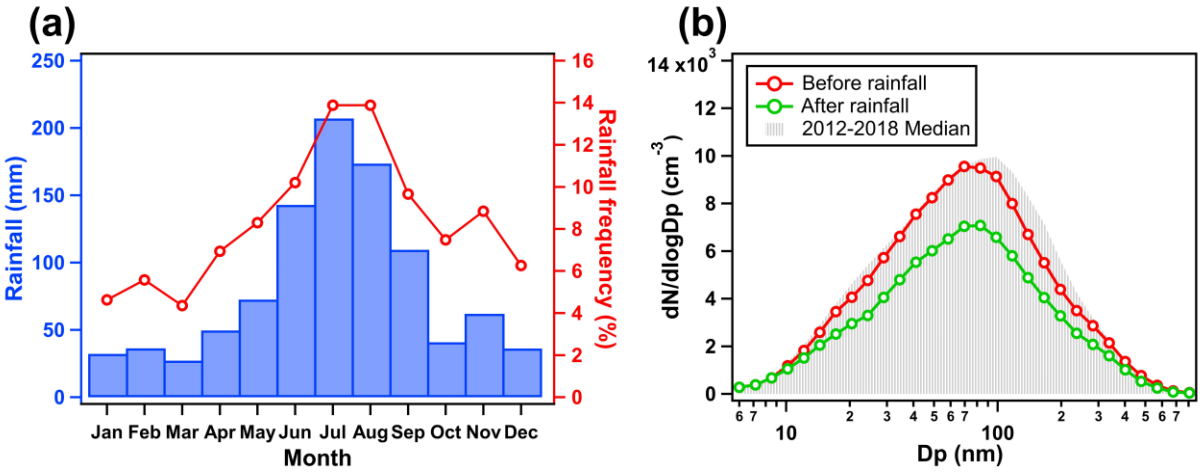

Figure 1. (a) Seasonal variations of accumulated precipitation (blue bar) and rainfall frequency (red line) observed at SORPES in 2012-2018. (b) The median PNSD (gray shaded area) in 2012-2018 and one hour before (red line) and after (green line) rainfall events.

Besides the PNSD data, this study used the water-soluble ions (WSI) data and carbon monoxide data, which were detected by the instrument for Measuring AeRosols and GAses (MARGA) and the trace gas monitor (ThermoTEI 48i), respectively. The meteorological parameters, including rainfall, air temperature, relative humidity (RH), wind speed, and wind direction, were obtained from the weather station (GRWS100) installed at the meteorological observation field of SORPES. In addition to the field measurements at SORPES, reanalysis and satellite retrievals, e.g. the European Centre for Medium-range Weather Forecasts Reanalysis v5 (ERA5) data and the Tropical Rainfall Measuring Mission (TRMM) 3B42 product, were used to support the analysis. The ERA5 data combines weather prediction simulations with observational data to provide accurate hourly meteorological conditions at 0.25°×0.25° spatial grid (Hersbach and Dee, 2016;Olauson, 2018). The TRMM 3B42 product provides precipitation estimates as a combination of different remote sensors set up in the satellite and has a temporal resolution of three hours and a spatial resolution of 0.25°×0.25°(Huffman et al., 2007).

2.2 Rainfall events selection criteria

In order to rule out other impacts except for rainfall on PNSD, all the rainfall episodes need to be screened to select suitable cases. Previous studies used some criteria for the selection of rainfall events (Blanco-Alegre et al., 2018;Cugerone et al., 2018;Geng et al., 2019;Laakso et al., 2003;Luan et al., 2019;Pryor et al., 2016;Roy et al., 2019;Wang et al., 2014), however, there is no uniform standard in the selection criteria. Here we summarized the selection criteria based on previous relevant studies as follows. Firstly, the rainfall events with sufficient precipitation are selected: (i) the accumulated rainfall no less than 0.4 mm, (ii) rainfall intensity no less than 0.3 mm h^{-1}, (iii) lasting at least 1 h, and (iv) at least 1-hour interval between each rainfall event. Secondly, as the change of meteorological conditions during rainfall events such as typhoon episodes and frontal passages can affect the particle number concentration, the meteorological selection criteria are needed to remove the effects of meteorological conditions changes: (i) the change in temperature at any adjacent hour during the rainfall events no greater than 6 ℃, (ii) the change in RH at any adjacent hour during the rainfall events no greater than 20%, (iii) the wind speed less than 4 m s^{-1} and (iv) the change in wind direction no more than 90° at the start and end of the rainfall event. The locally generated rainfall events were eliminated by the meteorological selection criteria, and thereby most of selected rainfall events were synoptic driven. According to the above screen criteria, 170 rainfall events among 382 rainfall events were selected. We tested the sensitivity of the chosen cut-points by reducing the cut-points of meteorological selection criteria by 20%. Stricter meteorological selection criteria do not affect the main results of this study. In this study, the selected 170 rainfall events are named as all events in the following discussion if not otherwise specified.

2.3 The calculation of below-cloud wet scavenging coefficient

The below-cloud wet scavenging coefficient (BWSC) shows the fraction of particles removed by rainfall in the unit of time. The basic equation of variation in the particle number concentration $c(d_p)$ due to rainfall scavenging is described by Eq. (1) (Seinfeld and Pandis, 2016):

$$\frac{dc(d_p)}{dt} = -\lambda c(d_p) \quad (1)$$

It is assumed that rainfall scavenging varies exponentially with time if no other processes (e.g. other sources or sinks of particles) are present during the rainfall event. d_p is aerosol particle diameter, and $\lambda(d_p)$ is the size-resolved scavenging coefficient given by Eq. (2)

$$\lambda(dp) = \int_0^\infty \frac{\pi}{4} D_p^2 U_t(D_p) E(D_p, d_p) N(D_p) dD_p, \quad (2)$$

where D_p is the raindrop diameter, U_t is the falling terminal velocity, $N(D_p)$ is the concentration of raindrops, and $E(D_p,d_p)$ is the collision efficiency between the raindrop and aerosol particle. As the collision efficiency, raindrop size distribution and raindrop velocity during the rainfall are difficult to observe, the theoretical scavenging coefficient is hard to obtain from the field measurements.

If the rainfall event occurs from t_0 to t_1, Eq.(1) can be integrated in time as follows (Laakso et al., 2003) :

$$\lambda(\mathrm{dp}) = -\frac{1}{t_1 - t_0}\ln\left(\frac{c_1(d_p)}{c_0(d_p)}\right). \quad (3)$$

In Eq. (3), $c_0(d_p)$ and $c_1(d_p)$ are the median particle number concentrations in each size bin before (t_0) and after (t_1) the rainfall event, respectively. In this study, we used Eq. (3) to calculate the scavenging coefficient and compared it with the theoretical estimation.

3 Results and Discussions

3.1 High BWSC events observed in eastern China

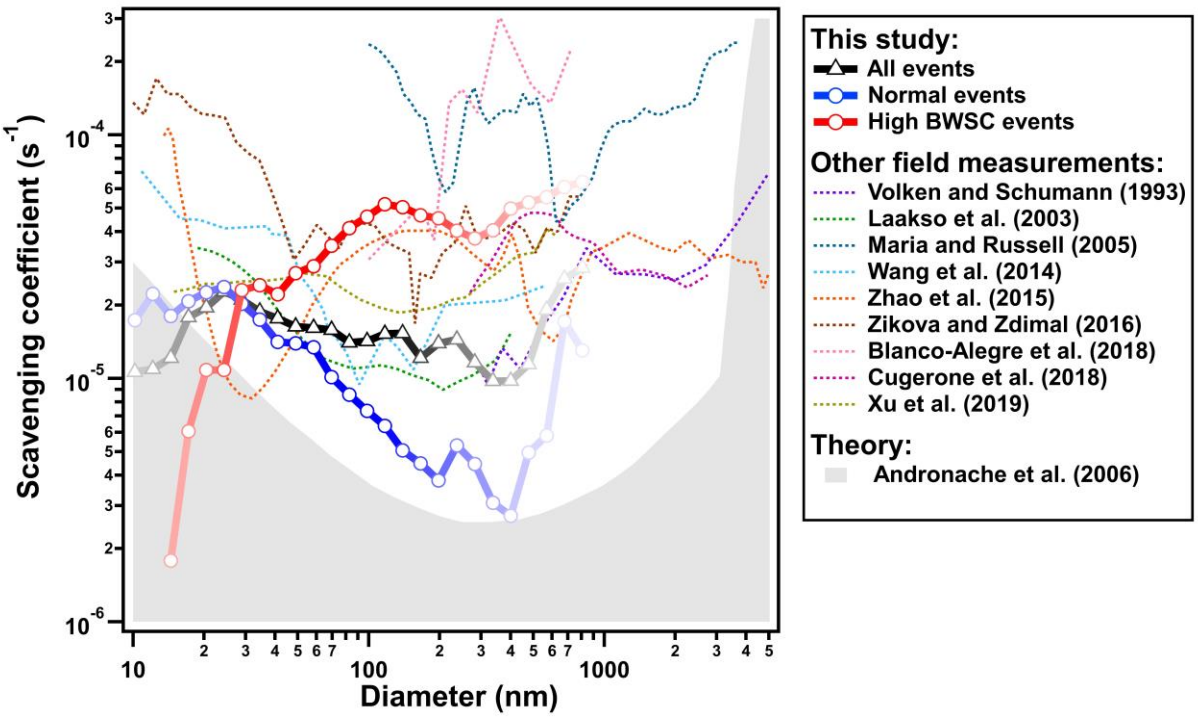

Figure 2. Below-cloud wet scavenging coefficients at SORPES station and the comparisons with other studies. The lines of this study are color coded with the particle number concentration in the corresponding size bin (color from light to dark represents the number concentration from low to high). Note that for theoretical values, the raindrop number size distribution is Marshall-Palmer distribution and rainfall intensity is set to be 10 mm/h (Andronache et al., 2006;Wang et al., 2010).

The BWSCs calculated in this study and the comparisons with other studies are shown in Fig. 2. The black line is the BWSC of all events at SORPES in YRD of eastern China, with color shade representing the particle number concentration in the corresponding size bins. The BWSC of all events at SORPES reaches a minimum in the 70-500

nm size range, but it is much higher than the theoretical value, which is similar to the results in Beijing, Mount Huang, Prague and southern Finland (Laakso et al., 2003;Wang et al., 2014;Xu et al., 2019;Zikova and Zdimal, 2016). Other studies observed higher BWSCs relative to theoretical value as well, although the BWSCs as well as the rain conditions differ from this study to some extent (Table 1) (Blanco-Alegre et al., 2018;Cugerone et al., 2018;Maria and Russell, 2005;Zhao et al., 2015;Volken and Schumann, 1993). In general, most of the BWSCs obtained from the field measurements have 1-2 orders of magnitude higher than the theory (Andronache et al., 2006;Wang et al., 2010). It is often considered to reduce this gap by adding extra below-cloud wet scavenging mechanisms to the theory. Bae et al. (2010) added electric charging and phoretic effects in the theoretical calculation, which made the discrepancy with measurements less. However, even with the additional mechanisms of below-cloud wet scavenging considered, the discrepancy between observation and theory is still large (Bae et al., 2010). Wang et al. (2010) proposed that the additional physical processes, such as cloud-aerosol microphysics, turbulent transport and mixing, could be the reasons for the large discrepancy between observed and theoretical BWSCs. In this study, we aim to understand this discrepancy from the perspective of the synoptic processes and air masses changing.

Table 1. BWSCs in corresponding particle size range and rainfall intensities observed in this study and other studies.

Size range (nm)	BWSC (s^{-1})	Rainfall intensity (mm h^{-1})	Note	Source
10-800	9.74×10^{-6}-2.84×10^{-5}	0.3-13.6	All events	This study
10-800	2.72×10^{-6}-2.37×10^{-5}	0.3-6.9	Normal events	This study
10-800	-8.15×10^{-6}-6.4×10^{-5}	0.3-13.6	High BWSC events	This study
10-510	7×10^{-6}-4×10^{-5}	0.94 (average)	Long-term data	Laakso et al., 2003
10-800	3.1×10^{-5}-1.5×10^{-4}	-	Long-term data	Zikova & Zdimal, 2016
13-750	1.08×10^{-5}-7.58×10^{-4}	0.9-15.79	Case study	Chate & Pranesha, 2004
100-4000	4.41×10^{-5}-2.39×10^{-4}	8	Case study	Maria & Russell, 2005
10-500	9.43×10^{-6}-7.08×10^{-5}	7	Case study	Wang et al., 2014
10-10000	7.48×10^{-6}-7.46×10^{-4}	1.57	Case study	Zhao et al., 2015
250-3000	2×10^{-5}-5×10^{-5}	0.40-2.04	Case study	Cugerone et al., 2018
14-740	1.86×10^{-5}-4.1×10^{-5}	0.28	Case study	Xu et al., 2019

Based on the variation of the particle number size distribution during the rainfall, we separated the well-screened rainfall events into two types: normal scavenging event and high BWSC scavenging event. The particle number concentrations in normal scavenging events (122 events, 72% of total events) show a moderate decreasing trend over

time (Fig. 3a). During the rainfall, the number concentration of small particles is first to decrease, after which the scavenging phenomenon gradually shifts to the size around 100 nm (Fig. 3a). It is consistent with the theory that the BWSC below 300 nm decreases as the particle size increases (i.e. the so-called "Greenfield gap"). Different from the normal scavenging events, the high BWSC events (48 events, 28% of total events) show a rapid decrease of particle number concentration in all size bins near the end of the rainfall (Fig. 3b). The BWSCs of high BWSC events reach a maximum between 70-300 nm, which largely exceeds the theoretical values as well as most of the previous observational studies. Changes in PNSD before and after rainfall events are more pronounced in high BWSC events than in normal scavenging events, with a significant change in dominant diameter from 100 nm to 50 nm in high BWSC events (Fig. S1). The extremely high BWSC values and a certain number of high BWSC events lead to overestimating the BWSC in the total events (Fig. 2). Table 1 compares the BWSCs in this study with other studies. In general, the normal scavenging events in this study have much lower BWSC than that in other studies, while the BWSC for all events is comparable with other studies. The BWSC becomes much closer to the theoretical value when high BWSC events are excluded. In the following sections, we will furtherly analyze the reasons for the high BWSC events.

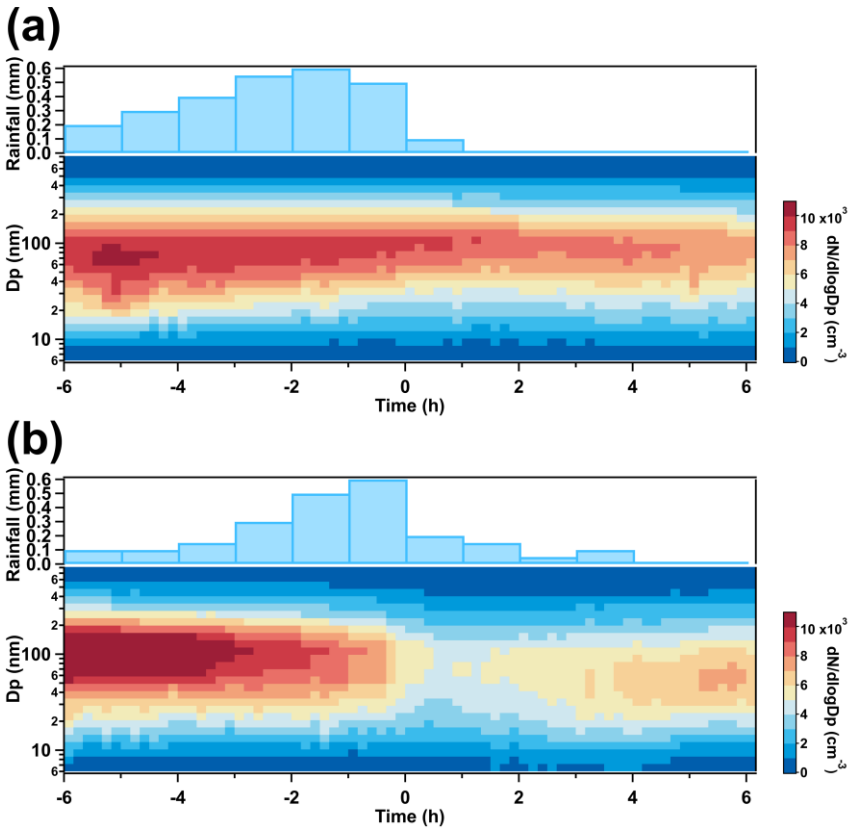

Figure 3. The variation of PNSD and precipitation for (a) normal scavenging events (the end of rainfall is marked as 0) and (b) high BWSC events (the time when the particle number concentration rapidly decrease is marked as 0).

215

3.2 Synoptic processes during high BWSC events

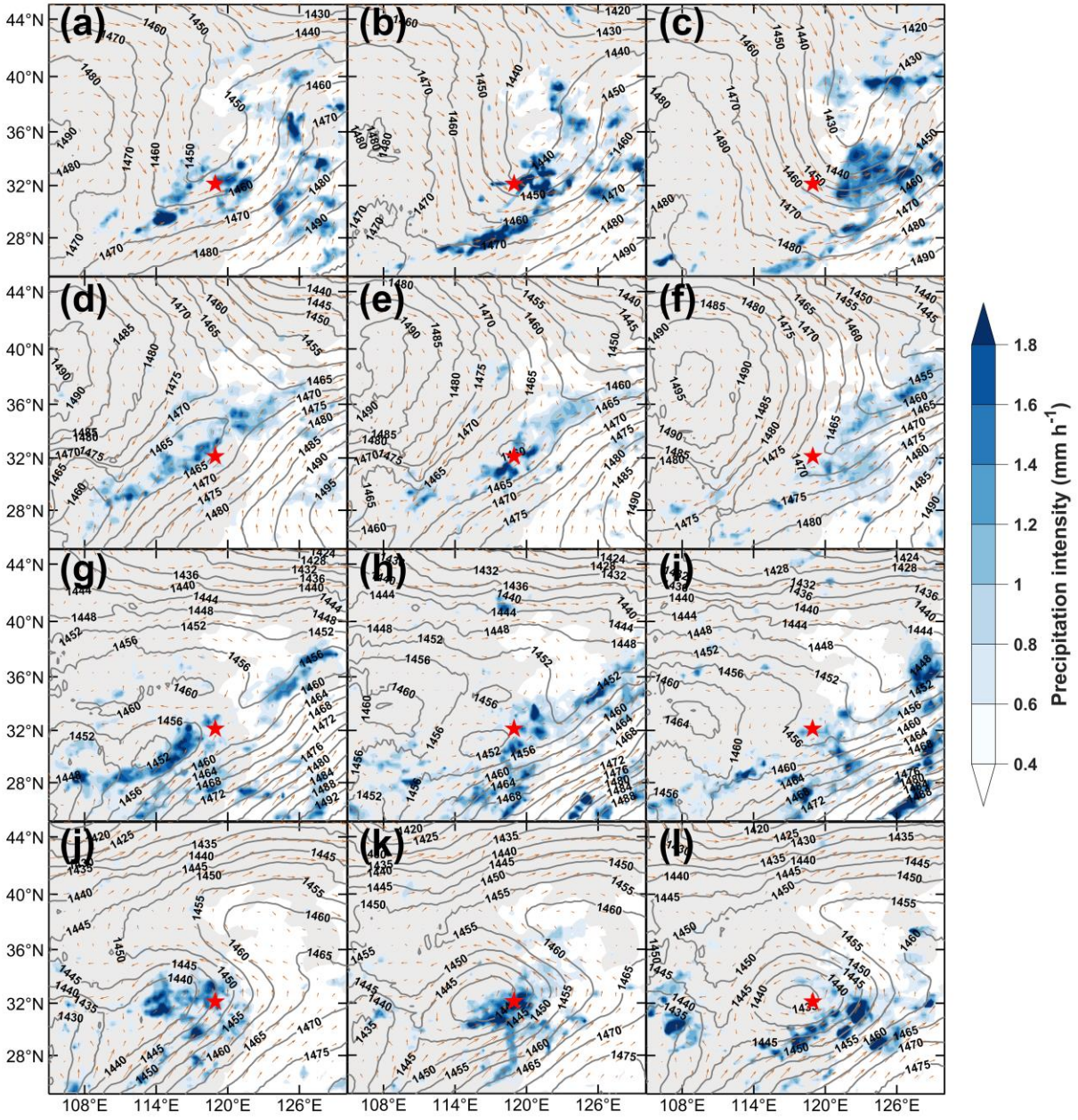

Figure 4. Distributions of winds and geopotential heights at 850 hPa and precipitation intensity before, at, and after the moment of sudden decrease in particle number concentration for (a-c) westerly trough type, (d-f) stationary front type, (g-i) vortex weakening type, and (j-l) vortex type. The red pentagram shows the location of SORPES station.

To investigate the reasons for the high BWSC events, we analyzed the synoptic processes during these events. Through subjective classification, the synoptic situation of high BWSC events can be divided into four main categories. When a trough moves from west to east, the synoptic situation is categorized as "westerly trough type" (16.6%); when a stationary front moves slowly at the SORPES station, the synoptic situation is categorized as "stationary front type" (31.3%); when a vortex weakens into the small trough at SORPES station, the synoptic situation is categorized as "vortex weakening type" (22.9%); when a vortex stays at SORPES station, the synoptic situation is categorized as "vortex type" (29.2%). The westerly trough type, stationary front type and vortex weakening type have clear movement of the synoptic systems, while the vortex type shows relatively stable circulations during the rainfall.

i) Westerly trough type

The rainfall events of this type are caused by the westerly trough, occurring mostly in spring and summer. Figures 4a-c show that the trough moves from west to east during the rainfall events. The rain belt is commonly located to the east of the westerly trough because this region is dominated by surface convergent winds, low pressure and ascending motion (Wallace and Hobbs, 2006). For rainfall events observed at the SORPES station, the SORPES station is located east of the westerly trough before the moment of the sudden decrease in particle number concentration and shifts to the west of the trough when the rainfall event is about to end. To further understand the transport characteristics of the air mass, we calculated the 3-day backward trajectories of air masses using Hybrid Single-Particle Lagrangian Integrated Trajectory (HYSPLIT) model (Draxler and Hess, 1998). Figure 5a shows the backward trajectory of air masses arriving at the SORPES station before, at and after the sudden decrease in particle number concentration. Consistent with the movement of the westerly trough, as shown in Fig 4a-c, the backward trajectories of air masses have a clockwise rotation during the rainfall event. Towards the end of the rainfall event, the air masses are mostly from the rainfall areas and have low particle number concentrations. This air mass transition explains the sudden decrease in particle number concentration for all the size bins. A typical case of type i high BWSC event, as well as the circulation evolvements and backward trajectories, is shown in Figures S2-S4.

ii) Stationary front type

The cold front events can be screened out by the meteorological criteria as described in section 2.2. However, the stationary front events, which occurred mostly in summer and autumn, cannot be excluded due to the slow movement of the synoptic systems. Figures 4d-f show that the stationary front moves slowly from northwest to southeast during the rainfall events at the SORPES station. The warm air mass climbs along the front to the cold side, accompanied by a drop in temperature, and the water vapor starts condensing (Wallace and Hobbs, 2006). Therefore, the rain belt is commonly near the front on the side of the cold air and moves with the front movement. The SORPES station is located on the warm side of the front before the rapid decrease of particle number concentration, while on the cold side of the front after that. Consistent with the movement of the stationary front (Fig 4d-f), the backward trajectories of the SORPES station switch from the YRD region to the northern area of the station. Towards the end of the rainfall event, the air masses are mostly from the rainfall areas and have low particle number concentrations. A typical case, as well as the circulation evolvements and backward trajectories, is shown in Figures S5-S7.

iii) Vortex weakening type

The rainfall events of this type are caused by a small trough, occurring mostly in summer and autumn. Figures 4g-i show that the vortex weakens into a small trough and moves from west to east during the rainfall events at the SORPES station. The rainfall areas are usually scattered ahead of the small trough (i.e. to the east of the trough in the westerly zone) because of the strong ascending motion in this area. The SORPES station is located ahead of the small trough during the rainfall event and shifts to the back of the small trough when the rainfall event is about to end. Unlike the first two types, backward trajectories of this type do not present horizontal rotation (Fig. 5c). However, when the rainfall is about to end, the origin of air mass gradually shifts from the ground to the high altitude due to the control of the descending motion air masses. Since, at high altitudes, the particle number concentrations are generally low (Qi et al., 2019), changes in the origin of air masses explain the sudden drop in particle number concentration. A typical case, as well as the circulation evolvements and backward trajectories, is shown in Figures S8-S10.

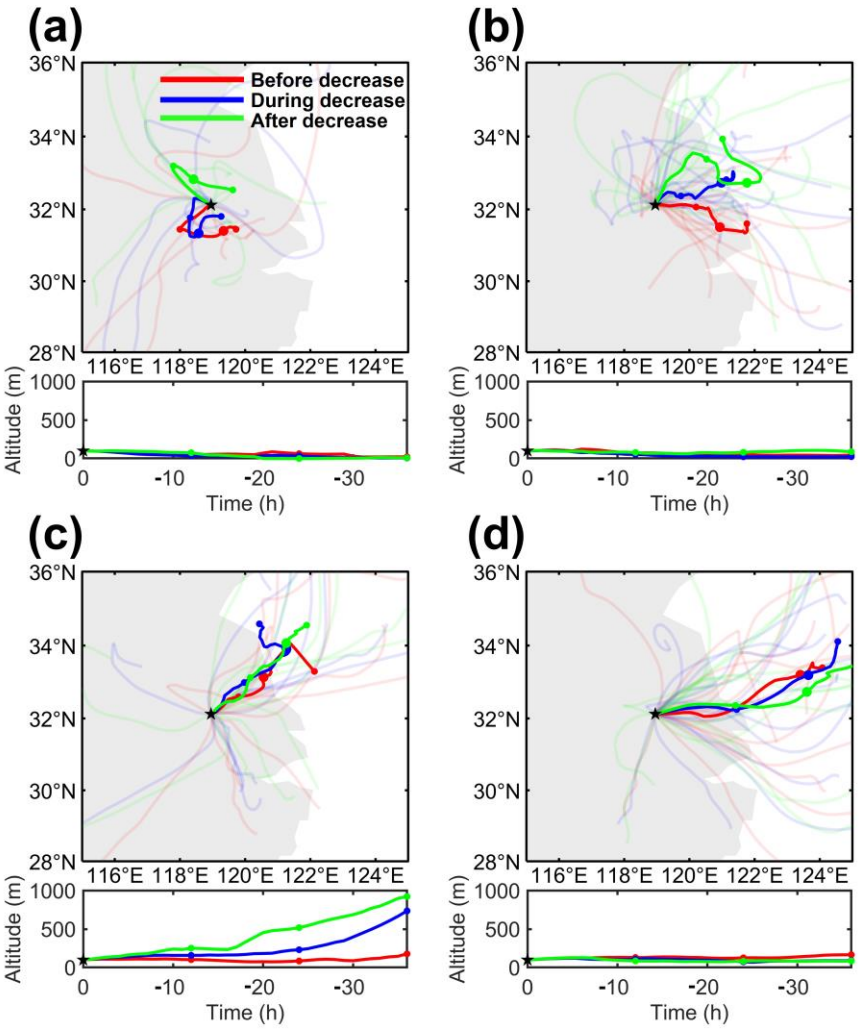

Figure 5. The backward trajectory before, at, and after the moment of sudden decrease in particle number concentration for (a) westerly trough type, (b) stationary front type, (c) vortex weakening type, and (d) vortex type.

iv) Vortex type

The rainfall events of this type are caused by the vortex, occurring mostly in spring and summer. The synoptic systems of the vortex type show no clear movement, which differs from other types. As shown in Fig 4j-l, the SORPES station is located on the eastern side of the vortex. The rainfall area moves from the western side of the SORPES station to the eastern side and covers the whole YRD region during the rainfall event. The air masses for the vortex type are mostly from the East China Sea and pass through the rain belt in the YRD region. Unlike other types, the backward trajectories of this type have no clear horizontal rotation or vertical height change (Fig. 5d), but the properties of air masses may still vary during the rainfall event. A typical rainfall event of vortex type, as well as the synoptic situation and backward trajectories, is shown in Figures S11-S13. The particle number concentration starts to decrease when the rainfall occurs but has a significant decrease in all the particle sizes, accompanied by the drop in carbon monoxide concentration during the rainfall. The simultaneous changes in the particle number concentration and carbon monoxide concentration indicate that the sudden decrease in particle number concentration is caused by the site being controlled by the marine air masses with minor influence from anthropogenic emissions in YRD.

In conclusion, the change of air masses is the main reason for the sudden decrease in particle number concentration during high BWSC events. It is worth noting that the transition of air masses is usually accompanied by changes in rainfall processes, e.g. the end of precipitation, which could easily mislead the calculation of BWSCs and cause the calculated BWSC to be much higher than the theory. Although the filtering procedures (see section 2.2) can screen some cases of significant air masses changes (e.g. cold front events, typhoon events), many more air masses transition cases with no obvious variations in meteorological parameters may not be screened.

3.3 The comparisons between high BWSC events and normal events

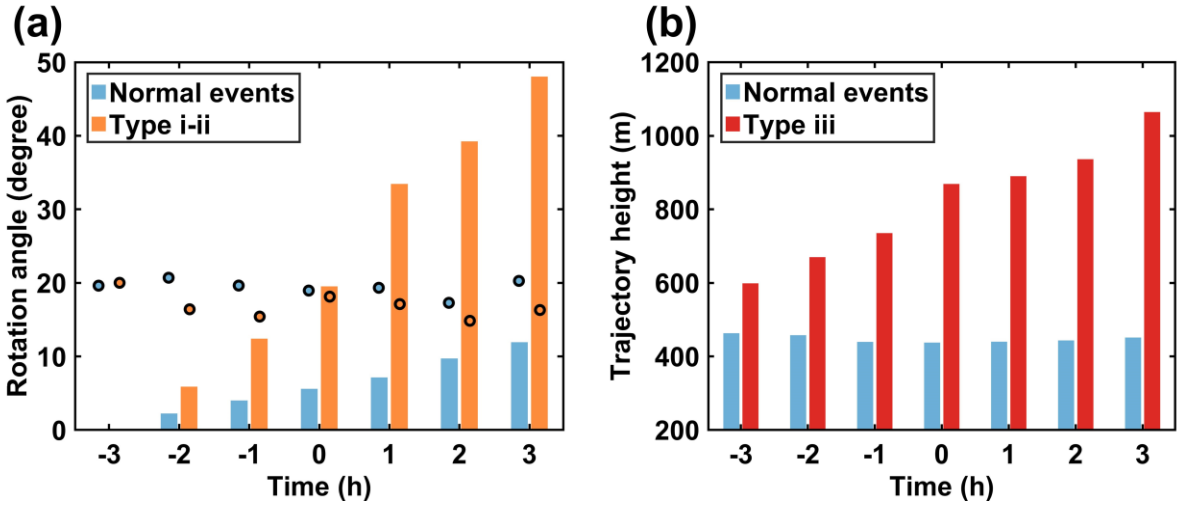

Figure 6. (a) The rotation angle of backward trajectory (bars) and wind direction (dots) during rainfall for normal event (blue) and type i-ii high BWSC events (orange). (b) The trajectory height (i.e. the maximum altitude of the 36-hour backward trajectory) during rainfall for normal event (blue) and type iii high BWSC events (red). Note that the

type iv high BWSC events were not plotted here due to the absence of clear horizontal rotation and vertical height changes in the backward trajectories.

To compare the high BWSC events with the normal events, we investigated the large-scale circulation patterns of the normal events as well. Through the subjective procedure, the circulation patterns of normal events could be mainly divided into three types, i.e. trough type (14.8%), vortex weakening type (34.4%) and vortex type (50.8%) (Fig. S14). Compared to high BWSC events, the circulation patterns for normal events do not change much during the rainfall. Consistent with the circulation pattern, the backward trajectories of air masses for the three types of normal events show minor variations during the rainfall (Fig. S15). Figure 6a shows the comparisons of the rotation angle of air mass trajectory and wind direction between type i-ii high BWSC events and normal events during rainfall. The air mass trajectory rotation angle of type i-ii high BWSC events varies more drastically than normal events, while the wind direction does not vary much in both types. It indicates that significant changes in the backward trajectories of air masses are not reflected in the wind direction observed at ground level, which explains why the type i-ii high BWSC events were not excluded by the selection criteria described in section 2.2. Figure 6b shows the differences in air masses trajectory height between type iii high BWSC events and the normal events. The trajectory height refers to the maximum altitude of the 36-hour backward trajectory. The backward trajectory height increases significantly in type iii high BWSC events, while it barely changes in the normal events. In general, the relatively stable circulation evolvements during normal events cause little changes in air masses, so the decrease in particle number concentration could be mainly attributed to the below-cloud wet scavenging.

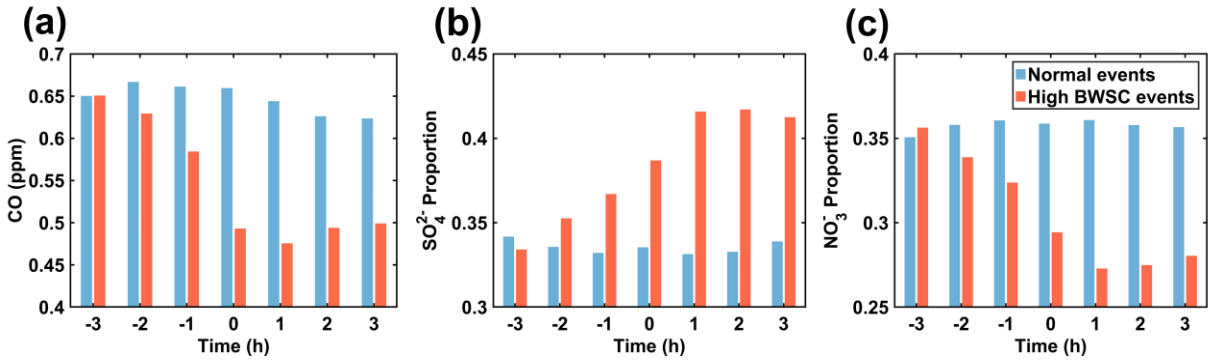

Figure 7. The comparisons of the variations of (a) carbon monoxide concentration, (b) the proportion of sulfate in water-soluble ions (WSI) and (c) the proportion of nitrate in WSI during normal scavenging events (blue) and high BWSC events (red).

The atmospheric components observed at the SORPES station can furtherly support that the origin of air masses changes during the high BWSC events. Figure 7a shows the differences in carbon monoxide concentration between high BWSC events and normal scavenging events. There is no significant change in carbon monoxide concentration

for normal scavenging events. As carbon monoxide is insoluble in water, wet scavenging can hardly induce significant changes in carbon monoxide. However, carbon monoxide concentration decreases significantly during the high BWSC events, suggesting changes in air masses. Figures 7b and 7c show the variations in the proportion of sulfate and nitrate in water-soluble ions (WSI) during high BWSC events and normal scavenging events. Similarly, the proportion of sulfate and nitrate in WSI changes indistinctively for normal scavenging events, while it changes significantly during the high BWSC events. The proportion of sulfate increases, and the nitrate decreases during the rainfall for the high BWSC events. To be concluded, in order to investigate the below-cloud wet scavenging based on field measurements, a detailed analysis of circulation patterns, air mass origins and atmospheric multi-components is required to select the episodes that are mainly affected by the below-cloud wet scavenging.

3.4 Factors influencing BWSCs

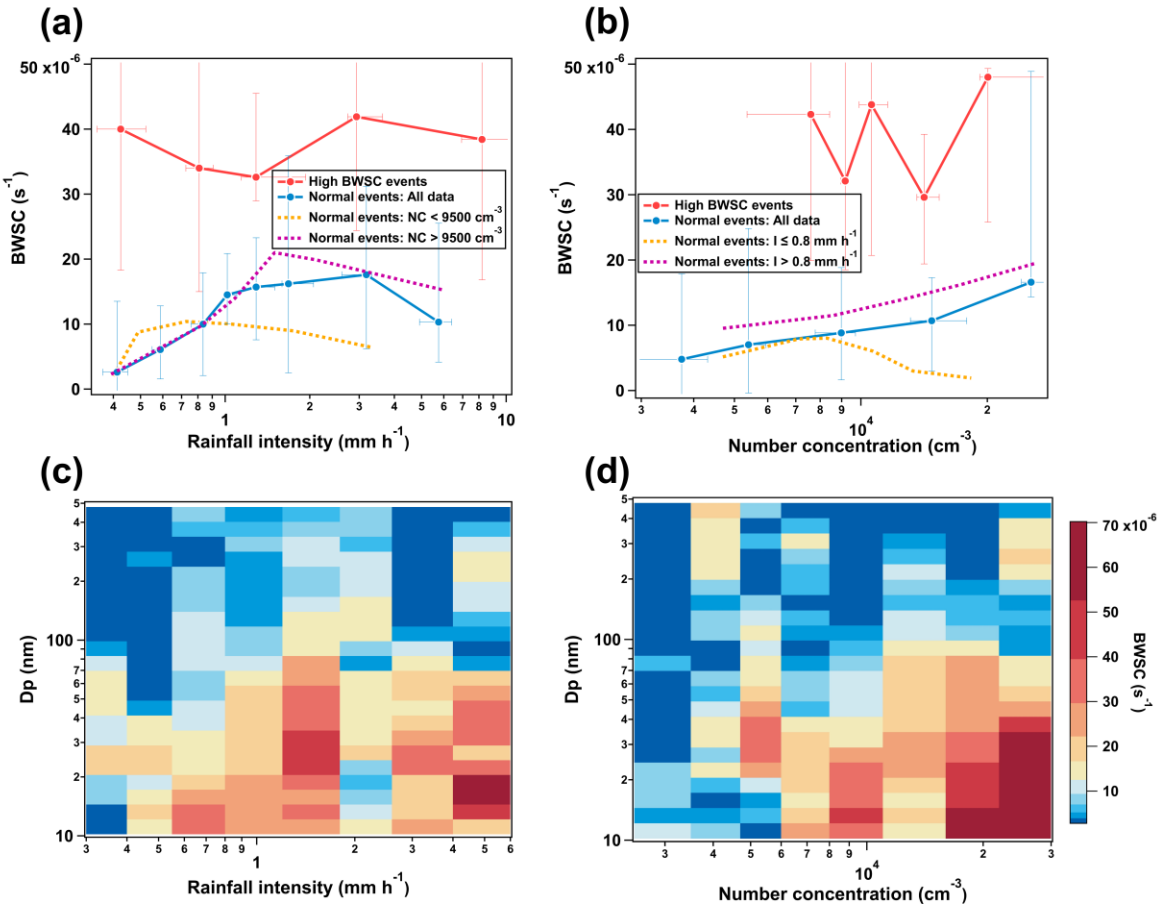

Figure 8. Below-cloud wet scavenging coefficients (median over particle sizes 10-500 nm) for high BWSC events and normal scavenging events as the function of (a) rainfall intensity and (b) particle number concentration prior to rainfall events. The dots represent the median and the error bars represent the upper and lower quartiles. Below-cloud wet scavenging coefficients in each size bin for normal scavenging events as the function of (c) rainfall intensity and (d) particle number concentration prior to rainfall events.

Previous studies found a close relationship between the rainfall intensity and BWSC and gave the parameterization between them (Blanco-Alegre et al., 2018;Chate and Pranesha, 2004;Laakso et al., 2003;Volken and Schumann, 1993;Wang et al., 2014;Xu et al., 2019). Figure 8a shows the relationship between the BWSC of total particles and rainfall intensity for high BWSC events and normal scavenging events observed at the SORPES station. As the scavenging of the high BWSC events is mainly caused by the change of air mass but not the wet deposition of raindrops, the BWSC for high BWSC events is not affected by the rainfall intensity. For normal scavenging events, the BWSC increases rapidly with rainfall intensity until the rainfall intensity reaches 1 mm h^{-1}, while at the rainfall intensity greater than 1 mm h^{-1}, the rate of the increase of BWSC with rainfall intensity slows down. This is because the BWSC is limited by the rainfall intensity under the low rainfall intensity condition while it switches to the limitation of background particle number concentration under high rainfall intensity conditions. The rainfall intensity turning point between two limitation intervals increases with the elevation of particle number concentration, which is around 1.5 mm h^{-1} at high number concentration and around 0.5 mm h^{-1} at low number concentration (Fig. 8a).

The particle number concentration before the rainfall events represents how many particles in the ambient can be scavenged by rain droplets. As shown in Fig. 8b, for normal scavenging events, there is a significant positive correlation between the BWSC and particle number concentration prior to the rainfall events, especially when the rainfall intensity is high. We furtherly investigate the dependence of BWSC on rainfall intensity and particle number concentration prior to the rainfall event for each size bin (Fig. 8c, d). The dependence of BWSC on rainfall intensity for particles below 100 nm (i.e. ultrafine particles) is similar with that of total particles (Fig. 8a, c), since the ultrafine particles dominate the particle number concentration at SORPES (Qi et al., 2015). The BWSCs are low for the particles larger than 100 nm due to the exist of "Greenfield" gap (Greenfield, 1957). Nevertheless, the increase in BWSC with increasing rainfall intensity can also be found for the particles larger than 100 nm. The dependence of BWSC on particle number concentration prior to rainfall event is obvious for ultrafine particles as well (Fig. 8d). Although the BWSCs are related to the particle size, the dependences of BWSCs on particle number concentration is uniform over all the size bins.

Theoretically, below-cloud wet scavenging is a 1st-order loss process and should not have the relationship with the particle number concentration prior to rainfall event (Eq. (1)). The particle number concentration varies exponentially with time if no other processes (other sources or sinks of particles) are present during the rainfall event (Fig. S16a). The slope of the line is the scavenging coefficient (i.e. λ in Eq. (1)) and does not vary with the particle number concentration prior to rainfall. However, in the real ambient environments, other processes such as particle formation, primary emissions, etc. cannot be excluded. For example, if there is a stable source of particles, the variation of particle number concentration will not vary exponentially by assuming consistent BWSC and formation rate. In field measurements, it is common to use Eq. (3) to calculate the BWSC. Although the actual BWSC is consistent, the calculated BWSC (dash lines in Fig. 16b) can increase with the increasing initial particle number concentration. Therefore, when parameterizing the BWSC with rainfall intensity based on field measurements, we need to not only carefully select the scavenging cases that are really caused by the wet scavenging (e.g. normal scavenging events in this study) but also take the other processes that influencing the PNSD into account (e.g. particle formation, primary emissions etc.).

4 Conclusions

Based on the long-term field measurements at the SORPES station in the Yangtze River Delta region of eastern China, we investigated the below-cloud wet scavenging of submicron particles in different size ranges in polluted environments. We find that 28% of total rainfall events are high BWSC rainfall events, commonly showing sudden decreases of particle number concentration in all size bins near the end of rainfall events. The high BWSC rainfall events cannot be screened out by the traditional filtering procedures based on meteorological parameters, which could contribute to much higher observed BWSCs due to the certain numbers of events. By investigating the simultaneously observed changes in carbon monoxide and aerosol chemical compositions during rainfall events, the circulation patterns and backward trajectories, we find the cause of high BWSC rainfall events is the air masses changing. The changes in air masses are accompanied by the end of rainfall events, which could easily mislead the calculation of BWSCs. The BWSCs for high BWSC events are not correlated with the rainfall intensity, which could then affect the parameterization of BWSC. After excluding the high BWSC events, we find the BWSC is not only correlated with the rainfall intensity but also the particle number concentrations prior to the rainfall events. The dependence of BWSC on the particle number concentrations is mainly caused by other processes except for wet scavenging that mislead the calculation of BWSC.

Through a careful review of previous literature, we found that the high BWSC events mentioned in this study can be observed not only in urban environments, but also in clean natural environments. This study highlights the discrepancy between the observed BWSC from field measurement and the theoretical value may not be as large as it is currently believed. When calculating the BWSCs based on field measurements, the impacts of air masses changing need to be carefully excluded. Long-term observations on multiple atmospheric components can help us to obtain the BWSCs that are truly caused by the below-cloud wet scavenging and update the parameterization in the numerical models. Moreover, rainfall events with specific circulation patterns could cause air masses changes. Thus, this study highlights accurate descriptions of the evolution of synoptic systems and the wet scavenging processes that are equally important for simulating air pollution in numerical models.

Data availability. The ERA5 reanalysis data is archived at the Copernicus Climate Change Service's Climate Data Store (http://cds.climate.copernicus.eu/). The TRMM 3B42 product is available at https://disc.gsfc.nasa.gov/datasets/TRMM_3B42_7/summary?keywords=TRMM%203B42. The measurement data at the SORPES station is available from the corresponding author upon request.

Author contributions. XQ and AD conceptualized the study. GN made the main data analysis with the supervision from XQ and AD. GN, LC, JW and XC conducted the measurements. GN and XQ wrote the original manuscript with contributions from all co-authors.

Competing interests. The contact author has declared that none of the authors has any competing interests.

Acknowledgments. We thank all the people and funds that have supported the long-term observations at the SORPES station. This work was in part undertaken in Joint International Research Laboratory of Atmospheric and Earth System Sciences and Jiangsu Provincial Collaborative Innovation Center for Climate Change, Nanjing University.

Financial support. This work was supported by the National Natural Science Foundation of China (42175113) and the Fundamental Research Funds for the Central Universities (14380191).

References

Andronache, C., Grönholm, T., Laakso, L., Phillips, V., and Venäläinen, A.: Scavenging of ultrafine particles by rainfall at a boreal site: observations and model estimations, Atmos. Chem. Phys., 6, 4739-4754, 10.5194/acp-6-4739-2006, 2006.

Asmi, A., Wiedensohler, A., Laj, P., Fjaeraa, A. M., Sellegri, K., Birmili, W., Weingartner, E., Baltensperger, U., Zdimal, V., Zikova, N., Putaud, J. P., Marinoni, A., Tunved, P., Hansson, H. C., Fiebig, M., Kivekäs, N., Lihavainen, H., Asmi, E., Ulevicius, V., Aalto, P. P., Swietlicki, E., Kristensson, A., Mihalopoulos, N., Kalivitis, N., Kalapov, I., Kiss, G., de Leeuw, G., Henzing, B., Harrison, R. M., Beddows, D., O'Dowd, C., Jennings, S. G., Flentje, H., Weinhold, K., Meinhardt, F., Ries, L., and Kulmala, M.: Number size distributions and seasonality of submicron particles in Europe 2008–2009, Atmos. Chem. Phys., 11, 5505-5538, 10.5194/acp-11-5505-2011, 2011.

Atkinson, R. W., Kang, S., Anderson, H. R., Mills, I. C., and Walton, H. A.: Epidemiological time series studies of $PM_{2.5}$ and daily mortality and hospital admissions: a systematic review and meta-analysis, Thorax, 69, 660-665, 10.1136/thoraxjnl-2013-204492, 2014.

Bae, S. Y., Jung, C. H., and Kim, Y. P.: Derivation and verification of an aerosol dynamics expression for the below-cloud scavenging process using the moment method, Journal of Aerosol Science, 41, 266-280, 10.1016/j.jaerosci.2009.11.006, 2010.

Blanco-Alegre, C., Castro, A., Calvo, A. I., Oduber, F., Alonso-Blanco, E., Fernández-González, D., Valencia-Barrera, R. M., Vega-Maray, A. M., and Fraile, R.: Below-cloud scavenging of fine and coarse aerosol particles by rain: The role of raindrop size, Quarterly Journal of the Royal Meteorological Society, 144, 2715-2726, 10.1002/qj.3399, 2018.

Calvo, A. I., Alves, C., Castro, A., Pont, V., Vicente, A. M., and Fraile, R.: Research on aerosol sources and chemical composition: Past, current and emerging issues, Atmospheric Research, 120-121, 1-28, 10.1016/j.atmosres.2012.09.021, 2013.

Chate, D. M., and Pranesha, T. S.: Field studies of scavenging of aerosols by rain events, Journal of Aerosol Science, 35, 695-706, 10.1016/j.jaerosci.2003.09.007, 2004.

Chate, D. M.: Study of scavenging of submicron-sized aerosol particles by thunderstorm rain events, Atmospheric Environment, 39, 6608-6619, 10.1016/j.atmosenv.2005.07.063, 2005.

Chen, L., Qi, X., Nie, W., Wang, J., Xu, Z., Wang, T., Liu, Y., Shen, Y., Xu, Z., Kokkonen, T., Chi, X., Aalto, P., Paasonen, P., Kerminen, V.-M., Petäjä, T., Kulmala, M., and Ding, A.: Cluster Analysis of Submicron Particle Number Size Distributions at the SORPES Station in the Yangtze River Delta of East China, Journal of Geophysical Research: Atmospheres, 126, 10.1029/2020JD034004, 2021.

Chen, R., Hu, B., Liu, Y., Xu, J., Yang, G., Xu, D., and Chen, C.: Beyond PM2.5: The role of ultrafine particles on adverse health effects of air pollution, Biochimica et Biophysica Acta (BBA) - General Subjects, 1860, 2844-2855, 10.1016/j.bbagen.2016.03.019, 2016.

Cugerone, K., De Michele, C., Ghezzi, A., and Gianelle, V.: Aerosol removal due to precipitation and wind forcings in Milan urban area, Journal of Hydrology, 556, 1256-1262, 10.1016/j.jhydrol.2017.06.033, 2018.

Daellenbach, K. R., Uzu, G., Jiang, J., Cassagnes, L.-E., Leni, Z., Vlachou, A., Stefenelli, G., Canonaco, F., Weber, S., Segers, A., Kuenen, J. J. P., Schaap, M., Favez, O., Albinet, A., Aksoyoglu, S., Dommen, J., Baltensperger, U., Geiser, M., El Haddad, I., Jaffrezo, J.-L., and Prévôt, A. S. H.: Sources of particulate-matter air pollution and its oxidative potential in Europe, Nature, 587, 414-419, 10.1038/s41586-020-2902-8, 2020.

Ding, A., Nie, W., Huang, X., Chi, X., Sun, J., Kerminen, V.-M., Xu, Z., Guo, W., Petäjä, T., Yang, X., Kulmala, M., and Fu, C.: Long-term observation of air pollution-weather/climate interactions at the SORPES station: a review and outlook, Frontiers of Environmental Science & Engineering, 10, 15, 10.1007/s11783-016-0877-3, 2016.

Ding, A. J., Fu, C. B., Yang, X. Q., Sun, J. N., Zheng, L. F., Xie, Y. N., Herrmann, E., Nie, W., Petäjä, T., Kerminen, V. M., and Kulmala, M.: Ozone and fine particle in the western Yangtze River Delta: an overview of 1 yr data at the SORPES station, Atmos. Chem. Phys., 13, 5813-5830, 10.5194/acp-13-5813-2013, 2013.

Downward, G. S., Nunen, E. J. H. M. v., Kerckhoffs, J., Vineis, P., Brunekreef, B., Boer, J. M. A., Messier, K. P., Roy, A., Verschuren, W. M. M., Schouw, Y. T. v. d., Sluijs, I., Gulliver, J., Hoek, G., and Vermeulen, R.: Long-Term Exposure to Ultrafine Particles and Incidence of Cardiovascular and Cerebrovascular Disease in a Prospective Study of a Dutch Cohort, Environmental Health Perspectives, 126, 127007, doi:10.1289/EHP3047, 2018.

Draxler, R., and Hess, G.: An overview of the HYSPLIT_4 modelling system for trajectories, Aust. Meteorol. Mag., 47, 1998.

Ge, B., Xu, D., Wild, O., Yao, X., Wang, J., Chen, X., Tan, Q., Pan, X., and Wang, Z.: Inter-annual variations of wet deposition in Beijing from 2014–2017: implications of below-cloud scavenging of inorganic aerosols, Atmos. Chem. Phys., 21, 9441-9454, 10.5194/acp-21-9441-2021, 2021.

Geng, T., Tong, H., Zhao, X., and Zhu, Y.: Effect of Wet Deposition on the Removal Efficiency of Particulate Matter in the Yangtze-Huaihe Region, Research of Environmental Sciences, 32, 273-283, 2019.

Greenfield, S.: Rain scavenging of radioactive particulate matter from the atmosphere, Journal of Meteorology, 14, 115-125, 1957.

Heal, M. R., Kumar, P., and Harrison, R. M.: Particles, air quality, policy and health, Chemical Society Reviews, 41, 6606-6630, 10.1039/C2CS35076A, 2012.

Hersbach, H., and Dee, D.: ERA-5 Reanalysis Is in Production, ECMWF Newsletter, No. 147, 2016.

Hou, P., Wu, S., McCarty, J. L., and Gao, Y.: Sensitivity of atmospheric aerosol scavenging to precipitation intensity and frequency in the context of global climate change, Atmos. Chem. Phys., 18, 8173-8182, 10.5194/acp-18-8173-2018, 2018.

Huffman, G. J., Bolvin, D. T., Nelkin, E. J., Wolff, D. B., Adler, R. F., Gu, G., Hong, Y., Bowman, K. P., and Stocker, E. F.: The TRMM Multisatellite Precipitation Analysis (TMPA): Quasi-Global, Multiyear, Combined-Sensor Precipitation Estimates at Fine Scales, Journal of Hydrometeorology, 8, 38-55, 10.1175/jhm560.1, 2007.

IPCC: Climate Change 2021: The Physical Science Basis. Contribution of Working Group I to the Sixth Assessment Report of the Intergovernmental Panel on Climate Change, Cambridge University Press, Cambridge, United Kingdom and New York, NY, USA, 2021.

Kerminen, V. M., Paramonov, M., Anttila, T., Riipinen, I., Fountoukis, C., Korhonen, H., Asmi, E., Laakso, L., Lihavainen, H., Swietlicki, E., Svenningsson, B., Asmi, A., Pandis, S. N., Kulmala, M., and Petäjä, T.: Cloud condensation nuclei production associated with atmospheric nucleation: a synthesis based on existing literature and new results, Atmos. Chem. Phys., 12, 12037-12059, 10.5194/acp-12-12037-2012, 2012.

Knibbs, L. D., Cole-Hunter, T., and Morawska, L.: A review of commuter exposure to ultrafine particles and its health effects, Atmospheric Environment, 45, 2611-2622, 10.1016/j.atmosenv.2011.02.065, 2011.

Kulmala, M., Kokkonen, T. V., Pekkanen, J., Paatero, S., Petäjä, T., Kerminen, V. M., and Ding, A.: Opinion: Gigacity – a source of problems or the new way to sustainable development, Atmos. Chem. Phys., 21, 8313-8322, 10.5194/acp-21-8313-2021, 2021.

Laakso, L., Grönholm, T., Rannik, Ü., Kosmale, M., Fiedler, V., Vehkamäki, H., and Kulmala, M.: Ultrafine particle scavenging coefficients calculated from 6 years field measurements, Atmospheric Environment, 37, 3605-3613, 10.1016/S1352-2310(03)00326-1, 2003.

Li, C., Bosch, C., Kang, S., Andersson, A., Chen, P., Zhang, Q., Cong, Z., Chen, B., Qin, D., and Gustafsson, Ö.: Sources of black carbon to the Himalayan–Tibetan Plateau glaciers, Nature Communications, 7, 12574, 10.1038/ncomms12574, 2016.

Luan, T., Guo, X., Zhang, T., and Guo, L.: The Scavenging Process and Physical Removing Mechanism of Pollutant Aerosols by Different Precipitation Intensities, Journal of Applied Meteorolgical Science, 30, 279-291, 2019.

Maria, S. F., and Russell, L. M.: Organic and Inorganic Aerosol Below-Cloud Scavenging by Suburban New Jersey Precipitation, Environmental Science & Technology, 39, 4793-4800, 10.1021/es0491679, 2005.

Ming, L., Jin, L., Li, J., Fu, P., Yang, W., Liu, D., Zhang, G., Wang, Z., and Li, X.: PM2.5 in the Yangtze River Delta, China: Chemical compositions, seasonal variations, and regional pollution events, Environmental Pollution, 223, 200-212, 10.1016/j.envpol.2017.01.013, 2017.

Olauson, J.: ERA5: The new champion of wind power modelling?, Renewable Energy, 126, 322-331, 10.1016/j.renene.2018.03.056, 2018.

Pryor, S. C., Joerger, V. M., and Sullivan, R. C.: Empirical estimates of size-resolved precipitation scavenging coefficients for ultrafine particles, Atmospheric Environment, 143, 133-138, 10.1016/j.atmosenv.2016.08.036, 2016.

Qi, X., Ding, A., Nie, W., Chi, X., Huang, X., Xu, Z., Wang, T., Wang, Z., Wang, J., Sun, P., Zhang, Q., Huo, J., Wang, D., Bian, Q., Zhou, L., Zhang, Q., Ning, Z., Fei, D., Xiu, G., and Fu, Q.: Direct measurement of new particle formation based on tethered airship around the top of the planetary boundary layer in eastern China, Atmospheric Environment, 209, 92-101, https://doi.org/10.1016/j.atmosenv.2019.04.024, 2019.

Qi, X. M., Ding, A. J., Nie, W., Petäjä, T., Kerminen, V. M., Herrmann, E., Xie, Y. N., Zheng, L. F., Manninen, H., Aalto, P., Sun, J. N., Xu, Z. N., Chi, X. G., Huang, X., Boy, M., Virkkula, A., Yang, X. Q., Fu, C. B., and Kulmala, M.: Aerosol size distribution and new particle formation in the western Yangtze River Delta of China: 2 years of measurements at the SORPES station, Atmos. Chem. Phys., 15, 12445-12464, 10.5194/acp-15-12445-2015, 2015.

Rosenfeld, D., Zhu, Y., Wang, M., Zheng, Y., Goren, T., and Yu, S.: Aerosol-driven droplet concentrations dominate coverage and water of oceanic low-level clouds, Science, 363, eaav0566, doi:10.1126/science.aav0566, 2019.

Roy, A., Chatterjee, A., Ghosh, A., Das, S. K., Ghosh, S. K., and Raha, S.: Below-cloud scavenging of size-segregated aerosols and its effect on rainwater acidity and nutrient deposition: A long-term (2009–2018) and real-time observation over eastern Himalaya, Science of The Total Environment, 674, 223-233, 10.1016/j.scitotenv.2019.04.165, 2019.

Schmale, J., Henning, S., Decesari, S., Henzing, B., Keskinen, H., Sellegri, K., Ovadnevaite, J., Pöhlker, M. L., Brito, J., Bougiatioti, A., Kristensson, A., Kalivitis, N., Stavroulas, I., Carbone, S., Jefferson, A., Park, M., Schlag, P., Iwamoto, Y., Aalto, P., Äijälä, M., Bukowiecki, N., Ehn, M., Frank, G., Fröhlich, R., Frumau, A., Herrmann, E., Herrmann, H., Holzinger, R., Kos, G., Kulmala, M., Mihalopoulos, N., Nenes, A., O'Dowd, C., Petäjä, T., Picard, D., Pöhlker, C., Pöschl, U., Poulain, L., Prévôt, A. S. H., Swietlicki, E., Andreae, M. O., Artaxo, P., Wiedensohler, A., Ogren, J., Matsuki, A., Yum, S. S., Stratmann, F., Baltensperger, U., and Gysel, M.: Long-term cloud condensation nuclei number concentration, particle number size distribution and chemical composition measurements at regionally representative observatories, Atmos. Chem. Phys., 18, 2853-2881, 10.5194/acp-18-2853-2018, 2018.

Seinfeld, J. H., and Pandis, S. N.: Atmospheric chemistry and physics: from air pollution to climate change, John Wiley & Sons, 2016.

Shen, Y., Virkkula, A., Ding, A., Luoma, K., Keskinen, H., Aalto, P. P., Chi, X., Qi, X., Nie, W., Huang, X., Petäjä, T., Kulmala, M., and Kerminen, V. M.: Estimating cloud condensation nuclei number concentrations using aerosol optical properties: role of particle number size distribution and parameterization, Atmos. Chem. Phys., 19, 15483-15502, 10.5194/acp-19-15483-2019, 2019.

Stier, P., Feichter, J., Kinne, S., Kloster, S., Vignati, E., Wilson, J., Ganzeveld, L., Tegen, I., Werner, M., Balkanski, Y., Schulz, M., Boucher, O., Minikin, A., and Petzold, A.: The aerosol-climate model ECHAM5-HAM, Atmos. Chem. Phys., 5, 1125-1156, 10.5194/acp-5-1125-2005, 2005.

Textor, C., Schulz, M., Guibert, S., Kinne, S., Balkanski, Y., Bauer, S., Berntsen, T., Berglen, T., Boucher, O., Chin, M., Dentener, F., Diehl, T., Easter, R., Feichter, H., Fillmore, D., Ghan, S., Ginoux, P., Gong, S., Grini, A., Hendricks, J., Horowitz, L., Huang, P., Isaksen, I., Iversen, I., Kloster, S., Koch, D., Kirkevåg, A., Kristjansson, J. E., Krol, M., Lauer, A., Lamarque, J. F., Liu, X., Montanaro, V., Myhre, G., Penner, J., Pitari, G., Reddy, S., Seland,

Ø., Stier, P., Takemura, T., and Tie, X.: Analysis and quantification of the diversities of aerosol life cycles within AeroCom, Atmos. Chem. Phys., 6, 1777-1813, 10.5194/acp-6-1777-2006, 2006.

Tinsley, B. A., Rohrbaugh, R. P., Hei, M., and Beard, K. V.: Effects of Image Charges on the Scavenging of Aerosol Particles by Cloud Droplets and on Droplet Charging and Possible Ice Nucleation Processes, Journal of the Atmospheric Sciences, 57, 2118-2134, 2000.

Twomey, S.: AEROSOLS, CLOUDS AND RADIATION, Atmospheric Environment Part a-General Topics, 25, 2435-2442, 10.1016/0960-1686(91)90159-5, 1991.

Volken, M., and Schumann, T.: A CRITICAL-REVIEW OF BELOW-CLOUD AEROSOL SCAVENGING RESULTS ON MT RIGI, Water Air and Soil Pollution, 68, 15-28, 10.1007/bf00479390, 1993.

Wallace, J. M., and Hobbs, P. V.: Atmospheric Science (Second Edition), Academic Press, 2006.

Wang, X., Zhang, L., and Moran, M. D.: Uncertainty assessment of current size-resolved parameterizations for below-cloud particle scavenging by rain, Atmos. Chem. Phys., 10, 5685-5705, 10.5194/acp-10-5685-2010, 2010.

Wang, Y., Zhu, B., Kang, H., Gao, J., Jiang, Q., and Liu, X.: Theoretical and observational study on below-cloud rain scavenging of aerosol particles, Journal of University of Chinese Academy of Sciences, 31, 306-313, 2014.

Wang, Y., Xia, W., Liu, X., Xie, S., Lin, W., Tang, Q., Ma, H.-Y., Jiang, Y., Wang, B., and Zhang, G. J.: Disproportionate control on aerosol burden by light rain, Nature Geoscience, 14, 72-76, 10.1038/s41561-020-00675-z, 2021.

Xausa, F., Paasonen, P., Makkonen, R., Arshinov, M., Ding, A., Denier Van Der Gon, H., Kerminen, V. M., and Kulmala, M.: Advancing global aerosol simulations with size-segregated anthropogenic particle number emissions, Atmos. Chem. Phys., 18, 10039-10054, 10.5194/acp-18-10039-2018, 2018.

Xie, Y., Ding, A., Nie, W., Mao, H., Qi, X., Huang, X., Xu, Z., Kerminen, V.-M., Petäjä, T., Chi, X., Virkkula, A., Boy, M., Xue, L., Guo, J., Sun, J., Yang, X., Kulmala, M., and Fu, C.: Enhanced sulfate formation by nitrogen dioxide: Implications from in situ observations at the SORPES station, Journal of Geophysical Research: Atmospheres, 120, 12679-12694, 10.1002/2015JD023607, 2015.

Xu, D., Ge, B., Wang, Z., Sun, Y., Chen, Y., Ji, D., Yang, T., Ma, Z., Cheng, N., Hao, J., and Yao, X.: Below-cloud wet scavenging of soluble inorganic ions by rain in Beijing during the summer of 2014, Environmental Pollution, 230, 963-973, 10.1016/j.envpol.2017.07.033, 2017.

Xu, D., Ge, B., Chen, X., Sun, Y., Cheng, N., Li, M., Pan, X., Ma, Z., Pan, Y., and Wang, Z.: Multi-method determination of the below-cloud wet scavenging coefficients of aerosols in Beijing, China, Atmos. Chem. Phys., 19, 15569-15581, 10.5194/acp-19-15569-2019, 2019.

Zhang, H., Yee, L. D., Lee, B. H., Curtis, M. P., Worton, D. R., Isaacman-VanWertz, G., Offenberg, J. H., Lewandowski, M., Kleindienst, T. E., Beaver, M. R., Holder, A. L., Lonneman, W. A., Docherty, K. S., Jaoui, M., Pye, H. O. T., Hu, W., Day, D. A., Campuzano-Jost, P., Jimenez, J. L., Guo, H., Weber, R. J., de Gouw, J., Koss, A. R., Edgerton, E. S., Brune, W., Mohr, C., Lopez-Hilfiker, F. D., Lutz, A., Kreisberg, N. M., Spielman, S. R., Hering, S. V., Wilson, K. R., Thornton, J. A., and Goldstein, A. H.: Monoterpenes are the largest source of summertime organic aerosol in the southeastern United States, Proceedings of the National Academy of Sciences, 115, 2038-2043, doi:10.1073/pnas.1717513115, 2018.

Zhao, S., Yu, Y., He, J., Yin, D., and Wang, B.: Below-cloud scavenging of aerosol particles by precipitation in a typical valley city, northwestern China, Atmospheric Environment, 102, 70-78, 10.1016/j.atmosenv.2014.11.051, 2015.

Zikova, N., and Zdimal, V.: Precipitation scavenging of aerosol particles at a rural site in the Czech Republic, Tellus Series B-Chemical and Physical Meteorology, 68, 10.3402/tellusb.v68.27343, 2016.